

Gap and pseudogap evolution within the charge-ordering scenario for superconducting cuprates

L. Benfatto, S. Caprara, and C. Di Castro

Dipartimento di Fisica - Università di Roma “La Sapienza” and Istituto Nazionale per la Fisica della Materia - Unità di Roma
 1, Piazzale Aldo Moro, 5 - 00185 Roma Italy

Received: date / Revised version: date

Abstract. We describe the spectral properties of underdoped cuprates as resulting from a momentum-dependent pseudogap in the normal state spectrum. Such a model accounts, within a BCS approach, for the doping dependence of the critical temperature and for the two-parameter leading-edge shift observed in the cuprates. By introducing a phenomenological temperature dependence of the pseudogap, which finds a natural interpretation within the stripe quantum-critical-point scenario for high- T_c superconductors, we reproduce also the $T_c - T^*$ bifurcation near optimum doping. Finally, we briefly discuss the different role of the gap and the pseudogap in determining the spectral and thermodynamical properties of the model at low temperatures.

PACS. 74.25.Dw Superconductivity phase diagrams – 71.10.Hf Non-Fermi-Liquid ground states, electron phase diagram and phase transitions in model systems – 74.20.Fg BCS theory and its developments

1 Introduction

The non-Fermi-liquid behaviour of the normal phase of the cuprates has two major features: (i) nearby optimum doping the in-plane resistivity is linear in T , signalling the absence of any other energy scale besides the temperature; (ii) in the underdoped regime photoemission and tunneling experiments show that a pseudogap persists well above

the critical temperature T_c up to a crossover temperature T^* [1]. While T_c increases with increasing doping, T^* starts from much higher values and decreases. The two temperatures merge around or slightly above optimum doping. Angle-resolved photoemission spectroscopy (ARPES) experiments indicate that the pseudogap and the superconducting gap have the same momentum dependence across T_c , which almost resembles a $d_{x^2-y^2}$ -wave,

namely $\Delta_{\mathbf{k}} = \Delta_0(\phi) \cos(2\phi)$, with $\phi = \arctan(k_y/k_x)$, and that both are tied to the underlying Fermi surface [2,3,4]. In the BCS d -wave approach Δ_0 is ϕ -independent and is proportional to T_c . Here instead $\Delta_0(\phi)$ is angle dependent and the ARPES spectra of the pseudogap state evolve smoothly and continuously in the superconducting ones across the critical temperature. A smooth evolution is also observed in tunneling spectra [5]. Moreover, the pseudogap at different \mathbf{k} points opens at different temperatures. At T^* a leading-edge shift (LE) appears in the ARPES spectra of underdoped Bi2212 for momenta near the $M \equiv (\pm\pi, 0); (0, \pm\pi)$ points of the Brillouin zone. The LE is observed as a finite minimum distance of the quasiparticle peak from the Fermi level in the non superconducting state, and leaves disconnected arcs of Fermi surface. When the temperature is lowered the LE regions around the M points enlarge and the arcs of Fermi surface reduce and shrink towards the nodal points of the corresponding d -wave superconducting gap below T_c . At the same time the doping dependence of the momentum structure of the LE is not trivial. As the doping is increased, the zero temperature LE at the M points, $\Delta_0(0)$, remains constant or decreases [2,3,4,7], while the LE around the nodal points $\Delta_0(\pi/4)$ seems to increase [4,6,7] and follow the rising of the critical temperature. Penetration depth measurements of the superfluid density $\rho_s(T)$ at low temperature probe the low-energy excitations around the nodal points in a d -wave superconductor, and therefore $\Delta_0(\pi/4)$. The correspondence between ARPES measurements of $\Delta_0(\pi/4)$ and the slope of $\rho_s(T)$ at $T = 0$

is made however more involved by the presence of the Landau renormalization factors [4].

Many theoretical models have been proposed to obtain a non-Fermi-liquid behaviour and to describe a pseudogap state. A firm result is however that above one dimension the Landau Fermi-liquid theory is generically stable and a strongly singular effective potential is required to disrupt it [8]. This result, together with the above phenomenology, suggests that a consistent description of the cuprates requires a strong momentum-, doping-, and temperature-dependent effective interaction. This interaction should affect the states near the M points of the Brillouin zone more effectively than along the diagonals and should have the temperature as the only energy scale around optimum doping. It was shown that in strongly correlated systems in the presence of additional attractive interactions (e.g. the Hubbard-Holstein model) and of long-range Coulomb forces, the exchange of quasi-critical charge (and spin) fluctuations provides such an effective electron-electron interaction both in the particle-particle and in the particle-hole channel [9]. Non-Fermi-liquid behaviour and strong pairing mechanism have in this way a common origin. These fluctuations arise near a finite-temperature instability line $T_{CDW}(\delta)$ for charge-density wave or stripe-phase formation, which ends in a quantum critical point (QCP) at $T = 0$ and $\delta = \delta_c$ near optimum doping [9,10]. As shown in Ref. [9], the effective electron-electron interaction near the charge instability has the form

$$V_{eff}(\mathbf{q}, \omega) \simeq \tilde{U} - \frac{V}{\kappa^2 + |\mathbf{q} - \mathbf{q}_c|^2 - i\gamma\omega}, \quad (1)$$

both in the particle-hole and particle-particle channels. Here $\mathbf{q} \equiv (q_x, q_y)$ and ω are the exchanged momenta and frequencies in the quasiparticle scattering, \tilde{U} is a residual repulsion, V is the strength of the attractive effective potential, \mathbf{q}_c is the critical wave-vector related to the charge ordering periodicity ($q_c = 2\pi/\lambda_c$). For physically relevant values of the parameters of the Hubbard-Holstein model \mathbf{q}_c turns out to be $(\pm 0.28, \pm 0.86)$ or equivalently $(\pm 0.86, \pm 0.28)$ [9]. In this case, therefore, \mathbf{q}_c connects the two branches of the FS around the M points and strongly affects these states. The mass term $\kappa^2 = \xi_c^{-2}$ is the inverse square of the correlation length of the charge order and provides a measure of the distance from criticality. This is given by $\delta - \delta_c$ in the overdoped region, by T in the quantum critical region around δ_c and by $T - T_{CDW}(\delta)$ in the underdoped region, where $T_{CDW}(\delta)$ sets in a new doping-dependent energy scale closely followed by $T^*(\delta)$. The characteristic time scale of the critical fluctuations is γ . The presence of a weak momentum-independent repulsion \tilde{U} together with a strong attraction of the order of $-V/\kappa^2$ in the particle-particle channel (cfr. Eq. (1) favors d -wave superconductivity approaching optimum doping from the overdoped regime, within direct BCS calculations [10]. In the underdoped regime we expect that precursor effects of charge ordering are relevant to the pseudogap formation and extend up to a temperature $T_0(\delta)$, (the mean field temperature for CDW formation) higher than $T_{CDW} \sim T^*$.

The two limiting cases when these precursors dominate the pseudogap formation in a single channel only (either

particle-particle or particle-hole channel) are simpler to analyze and each of them shows relevant aspects of the physics of the cuprates. The interplay of the two channels is an open problem still under investigation.

A first possibility is that the pseudogap opens due to incoherent pairing in the particle-particle channel, leading to a state where Cooper pairs around the M points are formed at $T^* \gtrsim T_{CDW}$ with strong long-wavelength fluctuations. Phase coherence, which characterizes a real superconducting state, is established at a lower temperature T_c , by coupling to the stiffness of the pairing near the nodal points [11].

In this paper we elaborate the other possibility, that the transition to the superconducting state takes place in the presence of a normal-state pseudogap parameter Δ_p resulting from interactions in the particle-hole channel. The issue arises of the interplay between the preformed pseudogap in the p-h channel and the additional pairing in the p-p channel. Having included most of the anomalous effects in the pseudogap formation, we determine T_c via the BCS approach for the pairing in the p-p channel. Our model originates as a simple schematization of a system interacting via the singular effective interaction (1) and is inspired to a similar model proposed by Nozières and Pistoiesi [12], with the inclusion of some specific aspects of the phenomenology of the cuprates. In Section 2 we discuss the model for the normal-state spectrum in presence of a pseudogap which has a d -wave form with amplitude Δ_p .

Assuming at the beginning a constant Δ_p , we discuss in Section 3 the general properties of our model, devoting

a particular attention to the doping and/or temperature dependence of T_c , of the LE and of the superfluid density.

In Section 4 we introduce a modulation for Δ_p , to take care of the δ -dependence of the new energy scale set by the $T_{CDW}(\delta)$ in the underdoped case. We assume that the pseudogap opens nearby a mean-field temperature $T_0(\delta)$ for the onset of CDW . $T_0(\delta)$ should follow the doping dependence of $T_{CDW}(\delta)$ in the underdoped regime and produce a variation in the density of states, as revealed by NMR and resistivity measurements on several compounds [1]. By a suitable fitting of $T_0(\delta)$, we give at the end a phenomenological description of the phase diagram of the cuprates, together with some physical quantities like the superfluid density, the specific heat and the leading edge.

2 The model

Within the above scenario, we describe the pseudogap in the normal state by means of a simplified model where a \mathbf{k} -dependent separation is present between a valence band and a conduction band, as a result of a \mathbf{k} -dependent effective interaction in the particle-hole channel. Differently from Ref. [12], we adopt a lattice electron model and assume that the pseudogap vanishes at some points of the Brillouin zone. Being interested on very qualitative aspects of the evolution of the pseudogap state, we shall mainly concentrate on a two-dimensional system related to the CuO_2 planes, the third dimension being relevant to establish the nature of the true transition and to cut off the corresponding fluctuations. Accordingly, we model

the normal-state spectrum as

$$\xi_{\eta\mathbf{k}} = -\mu + \eta\sqrt{\epsilon_{\mathbf{k}}^2 + \Delta_p^2\gamma_{\mathbf{k}}^2}, \quad (2)$$

where $\eta = +1(-1)$ in the conduction (valence) band, $\epsilon_{\mathbf{k}} = -2t(\cos k_x + \cos k_y)$ is the tight-binding dispersion law in the conventional metallic state (i.e. at $\Delta_p = 0$), Δ_p is the pseudogap parameter, and μ is the chemical potential. Δ_p governs together with the chemical potential the LE opening at the M points. The modulation of the pseudogap is given by the absolute value of $\gamma_{\mathbf{k}} = (\cos k_x - \cos k_y)/2$, which vanishes along the diagonals of the Brillouin zone. Since $\epsilon_{\mathbf{k}}$ vanishes along the lines $k_y = \pm(\pi \pm k_x)$, the two bands merge at the points $\mathbf{k}_P = (\pm\pi/2, \pm\pi/2)$. In the undoped system the LE has the \mathbf{k} -modulation given by the factor $\gamma_{\mathbf{k}}$. As the system is doped with respect to half-filling, a Fermi surface appears in the form of small pockets around the \mathbf{k}_P points. The LE , which vanishes along the Fermi surface, evolves thus continuously with respect to the undoped case. This is in contrast with the case of a \mathbf{k} -independent pseudogap Δ_p , which leads, in the lattice model, to a large Fermi surface in the doped system, with the chemical potential and the LE which evolve discontinuously with respect to half-filling.

We are aware of the fact that the complicated band structure of the cuprates is not simply fitted by the form (2). For instance, the band structure can be improved by extending the tight-binding expression beyond nearest neighbours. However, this does not represent a severe limitation to our approach, the generalization being straightforward. Moreover, the presence of the pseudogap leads, within our model, to the appearance of small pockets in

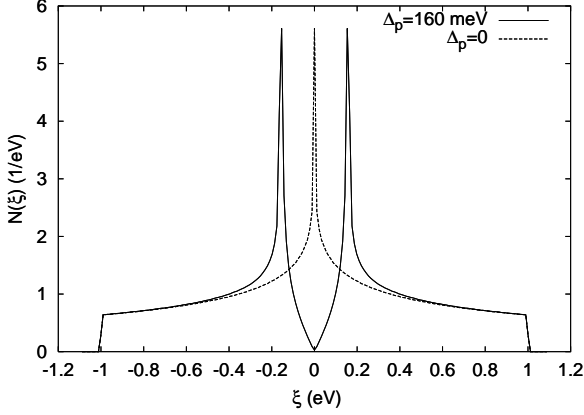


Fig. 1. Density of states at half-filling in the presence and in the absence of pseudogap for a hopping parameter $t = 0.25$ eV. Observe in the case $\Delta_p = 160$ meV the splitting of the van Hove singularity which gives rise to two peaks at energies $\xi \approx \pm\Delta_p$, with $\Delta_p \ll 2t$.

the weakly doped system. This issue is experimentally controversial, and it seems definitely confirmed that the two branches of each pocket, even when observed [13], are not equivalent [14]. However, the presence of pockets around the \mathbf{k}_P points, which result from the oversimplification of our description, is not essential to reproduce the finite LE observed in the single-particle ARPES spectra near the M points, and does not play any significant role in the forthcoming analysis. Therefore, we shall not further discuss this aspect.

The density of states corresponding to the band structure (2) vanishes only at $\xi = -\mu$, and is finite elsewhere, as shown in Fig. 1. The van Hove singularity which exists at $\xi = -\mu$ for $\Delta_p = 0$ is thus split into two singularities separated by $4t\Delta_p/\sqrt{(\Delta_p/2)^2 + 4t^2}$. For $\Delta_p \ll 2t$, as we shall assume in most of our calculation, the energy range where the density of states is suppressed is of order $2\Delta_p$.

Having included most of the effects of the anisotropic potential in the \mathbf{k} -dependence of the pseudogap $\Delta_p|\gamma_{\mathbf{k}}|$, for simplicity we assume that the onset of superconductivity is produced within a *BCS* approach by a constant pairing interaction among the carriers in the Cooper channel, apart again from a *d*-wave modulation. The relevance of the superconductive fluctuations of the phase of the order parameter will be discussed below, in parallel with the analysis of the properties of the superfluid density.

We introduce therefore an intraband interaction term between time-reversed states

$$H_I = -V\Omega \sum_{\eta} \int \frac{d^2k}{(2\pi)^2} \gamma_{\mathbf{k}} \gamma_{\mathbf{k}'} c_{\eta, \mathbf{k}\uparrow}^+ c_{\eta, -\mathbf{k}\downarrow}^+ \times \int \frac{d^2k'}{(2\pi)^2} c_{\eta, -\mathbf{k}'\downarrow} c_{\eta, \mathbf{k}'\uparrow}, \quad (3)$$

where V is the pairing strength, Ω is the volume of the system, $c_{\eta, \mathbf{k}, \sigma}^+$ is the creation operator of the electrons in the η -band, and the factors $\gamma_{\mathbf{k}}$ make the *d*-wave symmetry explicit. Introducing the order parameters $\Delta_{\eta} = V\langle \gamma_{\mathbf{k}} c_{\eta, \mathbf{k}\uparrow}^+ c_{\eta, -\mathbf{k}\downarrow}^+ \rangle$ we obtain the self-consistency equations

$$\Delta_{\eta} = \frac{V}{2} \int \frac{d^2k}{(2\pi)^2} \frac{\gamma_{\mathbf{k}}^2}{E_{\eta\mathbf{k}}} \tanh\left(\frac{\beta E_{\eta\mathbf{k}}}{2}\right) \Delta_{\eta} \quad (\eta = \pm 1) \quad (4)$$

$$\delta = 1 - \frac{1}{2} \sum_{\eta} \int \frac{d^2k}{(2\pi)^2} \left[1 - \frac{\xi_{\eta\mathbf{k}}}{E_{\eta\mathbf{k}}} \tanh\left(\frac{\beta E_{\eta\mathbf{k}}}{2}\right) \right], \quad (5)$$

where $E_{\eta\mathbf{k}} = \sqrt{\xi_{\eta\mathbf{k}}^2 + \Delta_{\eta}^2 \gamma_{\mathbf{k}}^2}$ is the quasiparticle energy in the superconducting state. The last equation fixes the chemical potential μ for any given doping δ with respect to half-filling. As most of the cuprates become superconducting by doping with holes, we study the hole-doped regime $\delta > 0$, where the chemical potential at $T = 0$, in the absence of pairing, falls in the valence band. Therefore, at weak-coupling, we find the solution $\Delta_{\eta=-1} = \Delta$,

$\Delta_{\eta=+1} = 0$ for Eq. (4). We point out that, due to the assumed band structure (2), the spectrum is particle-hole symmetric, and doping with electrons leads to the same self-consistent solution, provided the role of the two bands is interchanged.

Adding to the Hamiltonian (3) an interband interaction term, as discussed in Ref. [12], induces the $\Delta_{\eta=+1}$ to be different from zero even at weak-coupling. The two order parameters are generically different, contrary to the assumption of Ref. [12]. Indeed, the solution with one order parameter ($\Delta_{\eta=+1} = \Delta_{\eta=-1}$) has a higher free energy, which may become equal under very specific conditions.

3 General properties of the model

In this section we shall analyze the main outcomes of our model and their dependence on doping δ and on the temperature T . The parameters Δ_p and V at the beginning will be assumed to be temperature and doping independent, and not related to each other. This preliminary study allows us to point out the consequences of the assumed \mathbf{k} -dependent normal-state pseudogap, and to single out the regime of parameters suitable for a description of the phenomenology of the cuprates.

By solving the Eqs. (4)-(5) we obtain the temperature and doping dependence of the superconducting gap Δ and of the chemical potential μ , and we determine the phase diagram of the model in different physical regimes.

Before analyzing the two regimes of weak or strong coupling at various doping, we investigate the existence of a finite strength V_c of the interaction to have super-

conductivity in the undoped system, due to the fact that at half-filling the density of states vanishes at the Fermi energy. In our model, due to the d -wave nature of the preformed gap, the value of V_c is less than that found in Ref. [12] in presence of a constant gap. The equation that defines V_c at $T = 0$, $\delta = 0$ as a function of the pseudogap amplitude Δ_p is

$$\frac{2t}{V_c} = \frac{1}{2} \int \frac{d^2k}{(2\pi)^2} \frac{\gamma_{\mathbf{k}}^2}{\sqrt{(\cos k_x + \cos k_y)^2 + (\Delta_p/2t)^2 \gamma_{\mathbf{k}}^2}} \quad (6)$$

so that $V_c \approx \pi^2 \Delta_p/2$, for $\Delta_p \gg 2t$, and $V_c \sim 2t/\ln(4t/\Delta_p)$ for $\Delta_p \ll 2t$. The former limiting case is however not realistic: henceforth we shall definitely assume $\Delta_p \ll 2t$. Moreover, in the present scenario, the pseudogap is associated with scattering in the particle-hole channel. Pairing must therefore be absent at half-filling and we assume as the relevant regime for the cuprates $V < V_c$.

Critical temperature Within the BCS approach, the variation of the critical temperature with doping is controlled by the density of states at the Fermi level. At $\Delta_p = 0$, we recover the spectrum of a normal metal with nearest-neighbours hopping: at half-filling the Fermi energy is at the van Hove singularity, and T_c is maximum. By increasing doping, the density of states at the Fermi energy decreases, and so does T_c . This behaviour is excluded by the experiments. On the contrary, when $\Delta_p > 0$, the critical temperature is zero at half-filling (if $V < V_c$). At fixed finite doping, the critical temperature increases with increasing the pseudogap parameter Δ_p , reaches a maximum, and then decreases. By doping, the critical temperature follows the evolution of the density of states at the Fermi energy, reaching a maximum when the Fermi

energy passes through the boundary of the pseudogap region in the density of states, i.e. at the doping δ_{opt} such that $\mu \approx -\Delta_p$. For $\delta > \delta_{opt}$, T_c decreases with increasing doping. The resulting bell-shaped T_c vs δ curve captures the main features of the experimental results, as it will be more accurately presented in Section (4) with a doping dependent Δ_p .

The leading edge The quasiparticle spectrum, both in the normal and in the superconducting state, is characterized by a leading-edge shift LE , which is defined as $LE(\phi) = \min_{\eta, k} E_{\eta\mathbf{k}}$, where $\mathbf{k} = k(\cos \phi, \sin \phi)$ ¹. Due to the point symmetries of the system our analysis can be limited to the quadrant $0 \leq \phi \leq 45^\circ$. In the strong coupling regime the superconducting gap $\Delta \gg \Delta_p$, so the doping variation of Δ dominates the evolution of the zero-temperature LE at the M points, which increases approaching optimum doping, following T_c , in contrast with the behaviour observed in the experiments in the underdoped regime. In the weak-coupling regime instead the superconducting gap is much smaller than the pseudogap. For $\delta < \delta_{opt}$ the LE of the superconducting state is controlled by two independent parameters (see Fig. (2)), whose existence is also suggested by the combination of

¹ Within our mean-field treatment the excitations have a well defined energy and this quantity should be more correctly called ‘‘one-particle excitation gap’’. However, by using the term LE we want to put more emphasis on the distribution of spectral weight than on its coherent character, which is an artifact of our description of the cuprates in terms of a semiconducting band structure.

ARPES, penetration-depth and Andreev experiments [2, 3, 4, 6, 7]. The amplitude at the M points (LE_M) is given essentially by the value of the LE in the normal state, i.e.

$$LE_M = \frac{2t\Delta_p}{\sqrt{(\Delta_p/2)^2 + 4t^2}} - |\mu| \approx \Delta_p - |\mu| \quad (\Delta_p \ll 2t) \quad (7)$$

independent of T_c , whereas the slope at the nodes is $v_\Delta = \Delta_0(\phi = \pi/4) \propto \Delta \propto T_c$, in agreement with the experimental finding [4, 6, 7]. Note instead that $LE_M \approx \Delta$ for $\Delta_p = 0$.

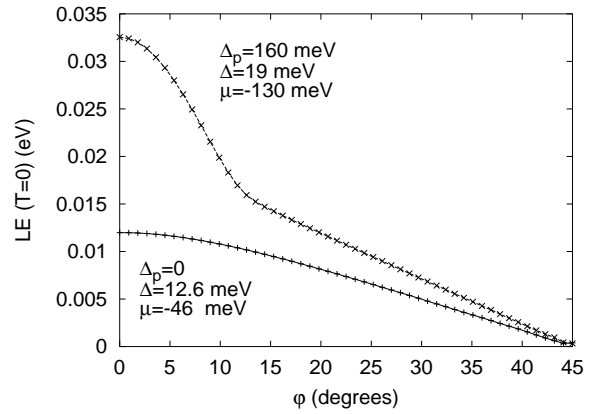


Fig. 2. Zero-temperature LE vs ϕ for $t = 250$ meV, $\delta = 0.1$, in the weak-coupling regime $V = 87$ meV, in the presence (\times) and in the absence ($+$) of the normal-state pseudogap Δ_p . Observe, for $\Delta_p = 160$ meV, the crossover around $\phi \approx 12^\circ$ to a regime dominated by the normal state pseudogap.

The variation of the chemical potential accounts now for the main dependence of the LE on doping. By increasing doping the normal-state LE_M , controlled by the pseudogap parameter Δ_p according to Eq. (7), decreases and vanishes at a doping δ_c . If Δ_p is doping independent (as we are assuming in this preliminary discussion), the δ_c for which $LE_M = 0$ coincides with the doping δ_{opt} for

the highest T_c . At $\delta > \delta_c$ the LE_M in the superconducting state is then given only by the superconducting order parameter Δ , as shown in Fig. 3. At fixed doping, the temperature variation of the LE depends on the closing of the superconducting gap at T_c , and eventually on the temperature dependence of Δ_p , if any (see Fig. 4).

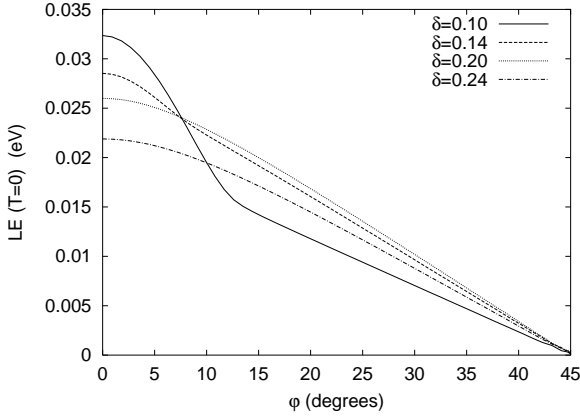


Fig. 3. Doping dependence of the zero temperature LE for $t = 250$ meV, $\Delta_p = 160$ meV and $V = 87$ meV. The $LE_M = LE(\phi = 0)$ decreases with increasing doping, due to the reduction of the normal-state LE_M given by Eq. (7). At $\delta > \delta_{opt} \approx 0.2$ the normal state LE closes and $LE(\phi, T = 0)$ is that of a standard d -wave superconductor (see also Fig. 2). Instead, the slope of the LE at the node $v_\Delta \propto \Delta$ increases before reaching δ_{opt} and then decreases. The critical temperature (proportional to $\Delta(T = 0)$ in the BCS approach) follows the same doping dependence.

The superfluid density In the superconducting phase the thermodynamic properties at low temperature are essentially determined by the quasiparticles near the nodes, i.e. by the superconducting gap Δ , whereas the pseudogap amplitude Δ_p plays no role. The superfluid density for instance can be evaluated according to the simple BCS

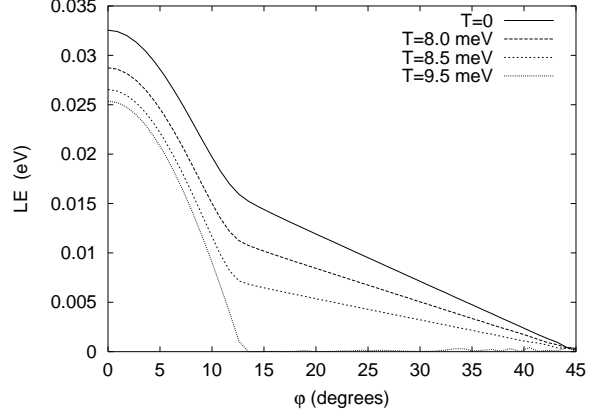


Fig. 4. Temperature dependence of the LE for the same set of parameters of Fig. 3 (increasing temperature from top to bottom). At $T > T_c = 9$ meV the superconducting gap closes, leaving a finite $LE_M \approx \Delta_p - |\mu|$.

formula:

$$\rho_s = \frac{1}{2} \sum_{\eta, l=x, y} \int \frac{d^2 k}{(2\pi)^2} \left\{ \frac{\partial^2 \xi_{\eta \mathbf{k}}}{\partial k_l^2} \left(1 - \frac{\xi_{\eta \mathbf{k}}}{E_{\eta \mathbf{k}}} \tanh \frac{\beta E_{\eta \mathbf{k}}}{2} \right) + 2 \left(\frac{\partial \xi_{\mathbf{k}}}{\partial k_l} \right)^2 \frac{\partial f(E_{\eta \mathbf{k}})}{\partial E_{\eta \mathbf{k}}} \right\}, \quad (8)$$

where $f(x)$ is the Fermi function. ρ_s decreases linearly in T at low temperature, as expected in a d -wave superconductor, with a slope determined only by the superconducting gap. For the assumed band dispersion (2) it can be shown that

$$\rho_s(T) - \rho_s(0) \simeq -\frac{T}{\Delta} \frac{16t \ln 2}{\pi}. \quad (9)$$

The slope of the superfluid density at low temperature, $\alpha = d\rho_s/dT(T = 0)$ is estimated in Ref. [4] by means of direct ARPES measurements of the slope v_Δ of the superconducting gap near the node. Because the observed v_Δ decreases in underdoped region (contrary to the gap at the M points), the doping dependence of $\alpha \propto 1/v_\Delta$ is found to increase by decreasing doping with respect to its optimum value. This behaviour is confirmed by our model: the slope

of $d\rho_s/dT$ given in Eq. (9) is controlled by the superconducting gap Δ , which follows the doping dependence of T_c in the underdoped regime. However, as observed in Ref. [4], the general trend of $\alpha(\delta)$, obtained by direct measurements of penetration depth, seems to be opposite, giving a decrease in the underdoped compounds of about 40% respect to its value at optimum doping. The correspondence between ARPES estimates and experimental data on $\alpha(\delta)$ requires the inclusion of doping dependent Landau renormalization factors, as discussed in Ref. [4] using the expression for ρ_s with the inclusion of quasiparticles interaction (see also Ref. [15]). The presence of a doping dependent Landau factor is plausible within our scenario if we attribute the origin of quasiparticle scattering to quasi-critical charge and spin fluctuations as in Eq. (1). The same holds for a correspondence between the slope of the density of states $N(\xi)$ near $\xi = 0$, where $N(\xi) \approx \eta\xi$ with $\eta \propto 1/v_\Delta$, and the values of η extracted by specific heat measurements [16].

As the temperature is increased, the system crosses over to a regime of higher energy excitations, which sample regions where $LE > \Delta$, and the slope is reduced. This can be seen in Fig. 5, where the temperature variation of $\rho_s(T)$ in weak and strong coupling is reported. The variation of the slope with respect to its low temperature value is less pronounced in the strong coupling case, where almost the same parameter controls the LE_M and the slope of the superconducting gap at the node.

Finally, we consider the doping dependence of the superfluid density. The variation of the $\rho_s(0)$ with doping is

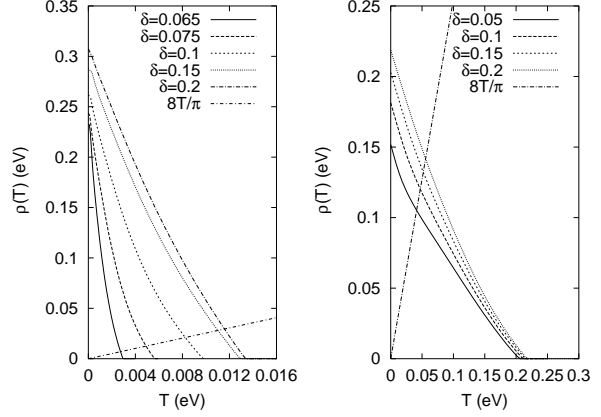


Fig. 5. $\rho_s(T)$ at different doping for $\Delta_p = 0.16$ eV, $t = 0.25$ eV in weak coupling ($V = 0.09$ eV, left) and strong coupling ($V = 0.9$ eV, right). The temperature at which the numerical curves intersect the line $8T/\pi$ is the T_{KT} , as explained in the text. Phase fluctuations are important between T_{KT} and T_{BCS} .

related to the variation of the number of carriers with doping: in a lattice model it does not increase monotonically, but reaches a maximum at an intermediate $0 < \delta < 1$, and then decreases. Nevertheless, the doping for the maximum $\rho_s(0)$ does not coincide necessarily with δ_{opt} .

The temperature dependence of the superfluid density allows us to give an estimate of the range of temperatures in which the phase fluctuations of the superconducting order parameter are relevant. Indeed, the critical temperature for phase coherence in a two-dimensional system, T_{KT} , is related to the phase stiffness ρ_s via the Kosterlitz-Thouless relation $\rho_s = 8T_{KT}/\pi$. Assuming the BCS temperature dependence for $\rho_s(T)$, the above relation becomes a self-consistency condition $\rho_s(T_{KT}) = 8T_{KT}/\pi$, and the phase fluctuations play an important role in the range of temperatures between T_{KT} and T_{BCS} . As it is naturally, in our model this region is very narrow

in weak coupling, and becomes larger and larger as the strength of the pairing interaction increases. Indeed while $\rho_s(0)$ mainly depends on the doping δ , T_{BCS} rapidly increases with increasing the coupling, and becomes much larger than T_{KT} . In Ref. [12], due to the discontinuity of the density of states at the band edges, at low doping a regime $T_c \gg T_{KT}$ is found. In such a case the transition is expected to be Kosterlitz-Thouless. In our model the density of states at the Fermi level vanishes smoothly and continuously as half-filling is approached. Therefore, in the weak-coupling limit, the critical temperature increases slowly with doping, and the Kosterlitz-Thouless regime is never found. Consistently with our assumptions within this model, in the regime of interest for cuprates, i.e. at weak coupling, the superconducting transition is essentially BCS-like, even in the underdoped region. The main part of the non classical behaviour is enforced by the presence of Δ_p .

Phase fluctuations effects have also been invoked to explain the linear- T behaviour of $\rho_s(T)$ [17]. Within a model with pseudogap formation in the p-p channel [11] these effects deserve a careful analysis.

4 Conclusions and discussion

In conclusion we want to summarize the previous results in closer connection with the phenomenology of the cuprates. The discussion of the previous section has given some preliminary indications on the set of parameters suitable to reproduce the general shape of the phase diagram observed in the cuprates. Nevertheless, to be consistent with

the experiments, we have to introduce the temperature and doping dependence of the pseudogap parameter $\Delta_p(T, \delta)$.

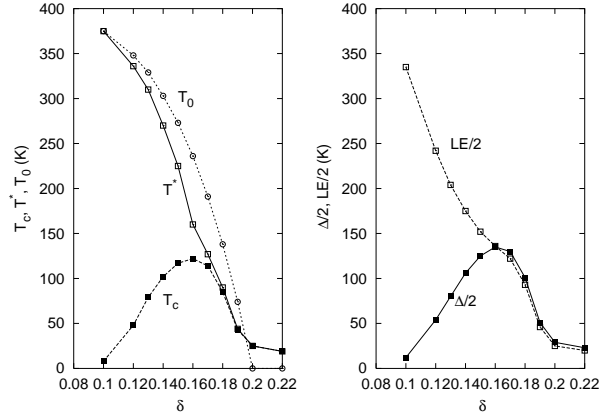


Fig. 6. Left panel: doping dependence of T^* , T_0 and of the critical temperature T_c . Right panel: doping dependence of the superconducting gap $\Delta(T = 0)$ and of the zero temperature LE_M . The set of parameters used is $t = 250$ meV, $V = 85$ meV, $c = 7$, $\delta_0 = 0.2$, and we assumed $T_0(\delta) = 40[1 - (\delta/\delta_0)^4]$ meV. The value of $T^*(\delta = 0) = T_0(\delta = 0)$ has been extrapolated from Ref. [2].

The mechanism for pseudogap formation has not been the main issue in this paper, which focuses on the properties of superconductivity arising in the pseudogap state. Nevertheless, according to the discussion of Sec. 1, we can imagine that $\Delta_p(T, \delta)\gamma_{\mathbf{k}}$ schematizes the whole complication of the strong scattering due to quasicritical charge fluctuations in the p-h channel, which arises in the stripe-QCP scenario [9]. We assume that the doping dependence of Δ_p follows the doping variation of the temperature T_0 ($T_0 > T^*$) at which a first variation in the density of states occurs, as revealed by NMR and resistivity measurements [1]. We adopt the simple relation:

$$\Delta_p(T, \delta) = cT_0(\delta)g(T/T_0(\delta)), \quad (10)$$

where $g(1) = 0$, $g(0) = 1$. $g(x)$ interpolates smoothly between these two limits² and c is a constant which we use as a fitting parameter. Since the identification of $T_0(\delta)$ via NMR and resistivity measurements leaves large uncertainty, we decide to refer to the ARPES experiments, which however only provide the temperature T^* of LE closure. We proceed in the following way. In the heavily underdoped regime the main temperature dependence of the LE_M (at fixed doping) is due to the decreasing of Δ_p with increasing the temperature, rather than to the temperature variation of the chemical potential. Then T^* and T_0 coincide at low doping in our model, whereas the experimental data seem to indicate that T_0 stays larger than T^* . This is an artifact of our approach, which is not devoted to establish the connection between the pseudogap state and the Mott insulator and/or the antiferromagnetic phase. This is a relevant open problem still under investigation. Meanwhile we put $T_0(\delta = 0) = T^*(\delta = 0)$ and extrapolating to $\delta = 0$ the $T^*(\delta)$ dependence reported in Ref. [2] for Bi2212 we obtain $T_0(\delta = 0) = 40$ meV. The constant c and the coupling V are adjusted to fix the values of the LE in the underdoped regime and the maximum T_c . The temperature T_0 is assumed to decrease with increasing doping and to vanish at $\delta_0 = 0.2$, slightly above

² Here we assume $g(x) = (1 - x^4/3)\sqrt{1 - x^4}$, which reproduces a mean-field-like behaviour near $T = 0$ and T_0 . However, the specific form of $g(x)$ does not play a crucial role in determining the general shape of the phase diagram.

the optimum doping, as expected in the QCP scenario [9].

Finally, we interpolate between $\delta = 0$ and δ_0 with the expression $T_0(\delta) = 40[1 - (\delta/\delta_0)^4]$ meV, which allows us to reproduce the shape of the curve $T^*(\delta)$ observed in the underdoped regime.

The resulting phase diagram is shown in Fig. 6. Even within a simplified description of the doping and temperature dependence of Δ_p , we recover the bifurcation of T^* and T_c observed in the underdoped regime, while they merge around optimum doping. T_c follows the typical bell-shaped curve as a function of δ . Our approach is still lacking of the temperature and doping dependence of the superconducting coupling, which plays an important role in determining the $T_c(\delta)$ variation around the QCP, as it has been shown elsewhere [9,10]. Even though the introduction of this further complication would definitively improve the agreement with the experimental data, with a faster decay of T_c at high doping, it would not change the main features of the pseudogap state obtained here. We reproduce the variation of the zero temperature LE_M in all the phase diagram: according to the general discussion of the previous section, the LE_M is determined by the normal state pseudogap in the underdoped region, and by the superconducting gap in the overdoped regime. As a consequence, in the underdoped regime the LE_M is uncorrelated to the characteristic energy scale of low temperature quasiparticle excitations, which probe the value of the superconducting order parameter around the nodal points. Having now a doping and temperature dependent Δ_p , the doping for the maximum T_c does not coincide any-

more with the doping at which the normal state leading edge closes, as we had in the presence of a constant Δ_p . Indeed, approaching optimum doping Δ_p itself closes at a lower temperature, and as a consequence the normal state LE_M closes faster than it would be under the only effect of the variation of the chemical potential with doping.

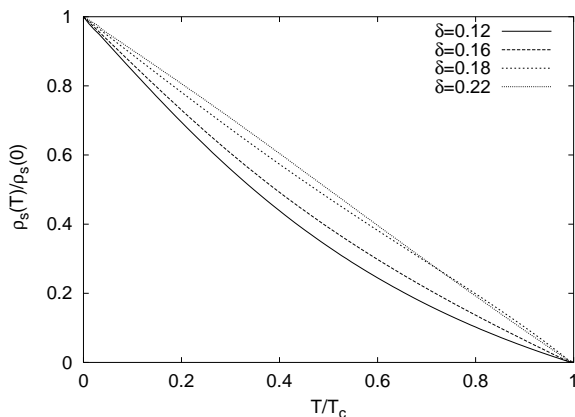


Fig. 7. Doping dependence of the normalized superfluid density $\rho_s(T)/\rho_s(0)$ as a function of T/T_c . We used the same set of parameters of Fig. 4. According to the phase diagram of Fig. 4, the optimum doping is at $\delta_{opt} \approx 0.16$. Observe that in the overdoped regime $\delta > \delta_{opt}$ the superfluid density has the standard d -wave mean field behaviour.

Finally, we report in Fig. 7 the normalized superfluid density $\rho_s(T)/\rho_s(0)$ as a function of T/T_c at various doping. In the overdoped regime, where the pseudogap closes, we recover the standard d -wave mean field result, which seems in a good agreement with experimental data [16] (see the curve for $\delta = 0.22$ in Fig. 7). However, in the underdoped region the dependence on doping of $d\rho_s/dT(T = 0)$ does not agree with the experiments as already discussed in Section (3), where the possible improvement due

to Landau factors has been addressed. We observe here another discrepancy: the slope of $\rho_s(T)$ near T_c in our model reduces by increasing the temperature contrary to the experimental findings [16]. As already indicated in Section (3), within our model the superconducting fluctuations are only important in the short region between T_{KT} and T_{BCS} . The inclusion of these fluctuations, by reducing ρ_s near T_c , would at least partially take care of this discrepancy.

Even though we did not reach yet the point to exploit fully the momentum and doping dependence of a quasi-singular effective interaction among quasiparticles arising nearby an instability in the p-p and p-h channels, altogether within the present simplified approach we produce a behaviour of $T_c(\delta)$, of $T^*(\delta)$ and of the $LE_M(0, \delta)$ in reasonable agreement with the experimental findings.

Acknowledgements

We acknowledge A. Perali, C. Castellani, and M. Grilli for helpful discussions.

References

1. For a recent review see, e.g., T. Timusk and B. Statt, Rep. Prog. Phys. **62**, 61 (1999).
2. H. Ding *et al.*, Nature **382**, 51 (1996); H. Ding *et al.* J. Phys. Chem. Solids **59**, 1888 (1998).
3. M. R. Norman *et al.*, Nature **392**, 1587 (1998).
4. J. Mesot *et al.*, Phys. Rev. Lett. **83**, 840 (1999).

5. Ch. Renner *et al.*, Phys. Rev. Lett. **80**, 149 (1998). N. Miyakawa *et al.*, Phys. Rev. Lett. **80**, 157 (1998).
6. C. Panagopoulos and T. Xiang, Phys. Rev. Lett. **81**, 2336 (1998).
7. G. Deutscher, Nature **397**, 410 (1999).
8. C. Castellani and C. Di Castro, Physica A **263**, 197 (1999), and references therein.
9. C. Castellani, C. Di Castro, and M. Grilli, Phys. Rev. Lett. **75**, 4650 (1995); Z. Phys. B **103**, 137 (1997).
10. A. Perali, C. Castellani, C. Di Castro, and M. Grilli, Phys. Rev. B **54**, 16216 (1996).
11. A. Perali, *et al.*, cond-mat/9912363, C. Castellani, *et al.*, cond-mat/0001231
12. P. Nozières and F. Pistolesi, Eur. Phys. J. B **10**, 649 (1999).
13. N. L. Saini, *et al.* Phys. Rev. Lett. **79**, 3467 (1997). S. La Rosa, *et al.* Solid State Commun. **104**, 459 (1997). P. Aebi, *et al.* Phys. Rev. Lett. **72**, 2757 (1994)
14. S. V. Borisenko, *et al.*, cond-mat/9912289
15. A. J. Millis, *et al.* J. Phys. Chem. Solids **95**, 1742 (1998).
16. C. Panagopoulos, *et al.*, Phys. Rev. B **60**, 14617 (1999).
17. E. W. Carlson, *et al.* Phys. Rev. Lett. **83**, 612 (1999)